

THE PHYSICAL REVIEW

A journal of experimental and theoretical physics established by E. L. Nichols in 1893

SECOND SERIES, VOL. 185, No. 1

5 SEPTEMBER 1969

K-Shell Auger Transition Rates and Fluorescence Yields for Elements Be-Ar

Eugene J. McGuire*

Sandia Laboratory, Albuquerque, New Mexico 87115

(Received 13 March 1969)

The quantity $-rV(r)$ for ions, formed by removing a 1s electron from the neutral atom, is computed by the approach of Herman and Skillman. A straight-line approximation of $-rV(r)$ is made, leading to an exactly solvable one-electron Schrödinger equation. The discrete and continuum orbitals are used to compute Auger *KLL* and *KLM* transition rates, radiative rates, and fluorescence yields for the elements Be-Ar. Comparison with experimental *K*-shell fluorescence yields indicates the calculations are 25% too high for Mg and Al and within 5% for Ar. Comparison of the individual Auger transition intensities for F, Ne, Na, and Mg indicates differences of 50%. This 50% difference between calculated and measured individual Auger transition intensities persists up to Ar, where the sum of the individual intensities is in better than 7% agreement with that derived from the fluorescence yield and *K*-state width.

I. INTRODUCTION

Though the Auger effect¹ has long been understood, and the theoretical formalism² for the calculation of Auger transition rates has long been available, there have been few systematic attempts to calculate absolute Auger rates, and the related property, the atomic fluorescent yield. Callen³ has computed *KLL* Auger rates for the elements from $Z=1$ to $Z=80$. However, they were calculated using screened hydrogenic wave functions and appear significantly in error for the lighter elements (when compared⁴ to experiment or to the modified Hartree calculation

of Rubenstein⁵ for Ar).

In this paper, we report calculations of Auger transition rates and fluorescent yields for an initial *K*-shell hole in the elements Be-Ar. We use the formalism of Burhop² in *L-S* coupling. In the radial integrals, we use one-electron orbitals determined by the same procedures as in recently reported photoionization calculations.⁶ In Sec. II, we briefly discuss the formalism and the reduced matrix element, and in Sec. III, the orbitals used. In Sec. IV, we report the calculated total Auger rates, radiative rates, and fluorescence yields. In Sec. V, we compare calculated individual Auger rates with measurements.

II. AUGER RATES

In Burhop's formalism² the Auger transition process is treated in time-dependent perturbation theory, with the interaction between two electrons as the perturbation. One then approximates the initial- and final-state wave function as a product of one-electron orbitals. With this approximation and the unrelaxed core approximation [e.g., the 1s orbital in $(1s)^1$ in the initial state is identical to the 1s orbital in $(1s)^2$ in the final state], one can reduce the matrix element to a double integral involving four orbitals. The double integral is multiplied by a factor arising from integration over angles. For Auger transitions from ions composed of completely filled shells plus either an *s* or a *p* vacancy, one can find the above proce-

dure worked out in Rubenstein's thesis.⁵

For initially filled shells plus a K -shell vacancy, the relevant rates in inverse atomic time units (1 atu = 2.42×10^{-17} sec) are

$$A_A(s, s') = 4\pi f \times \frac{1}{2} \{3[R_0(0, 0, s, s') - R_0(0, 0, s', s)]^2 + [R_0(0, 0, s, s') + R_0(0, 0, s', s)]^2\},$$

$$A_A(s, p) = 4\pi f \times \frac{3}{2} \{3[R_0(0, 1, s, p) - \frac{1}{3}R_1(0, 1, p, s)]^2 + [R_0(0, 1, s, p) + \frac{1}{3}R_1(0, 1, p, s)]^2\},$$

$$A_A(p, p') = 4\pi f \times \frac{1}{6} \{3[R_1(0, 0, p, p') - R_1(0, 0, p', p)]^2 + [R_1(0, 0, p, p') + R_1(0, 0, p', p)]^2 \\ + 6[R_1(0, 2, p, p') - R_1(0, 2, p', p)]^2 + 2[R_1(0, 2, p, p') + R_1(0, 2, p', p)]^2\},$$

where the radial integral

$$R_K(l_a, l_b, l_c, l_d) = \iint r_1^2 dr_1 r_2^2 dr_2 \psi_{l_a}(r_1) \psi_{l_b}(r_2) [(r^<)^K / (r^>)^{K+1}] \psi_{l_c}(r_1) \psi_{l_d}(r_2). \quad (1)$$

The factor f is 1 if the electrons are inequivalent and $\frac{1}{2}$ if they are equivalent. The factor 4π arises from the difference in the normalization of the continuum orbital in Ref. 6 from that in Chap. 14 of Mott and Massey.⁷

For transitions in which one or two electrons come from a partially filled shell, the reduction of the matrix element in Ref. 5 must be modified by the introduction of fractional parentage coefficients.⁸ The author⁹ has done this for L - S coupling. The expression for the transition rate between terms of the initial and final configurations is elaborate. However, for the fluorescence yield one averages over the initial-configuration terms and sums over the final-configuration terms. The result can be stated as: If initially, one has n electrons in a shell that could contain n_0 electrons, and if one of the n electrons is involved in the Auger process use the full-shell rate reduced by n/n_0 . Further, if two of the n electrons are involved in the Auger process use the full-shell rate reduced by $n(n-1)/n_0(n_0-1)$.

For the radiative transition probability, we used¹⁰

$$A_R = 1.94 \times 10^{-7} N f n p, 1s(\Delta E)^2, \quad (2)$$

where $f n p, 1s$ is the oscillator strength per electron, N is the number of electrons initially in the $n p$ shell, and ΔE is the energy of the radiative transition in Ry (13.6 eV).

The fluorescence yield is given by

$$\omega_K = \sum A_R / (\sum A_A + \sum A_R).$$

III. ONE-ELECTRON ORBITALS AND RADIAL INTEGRAL

The one-electron orbitals used in Eq. (1) were found by approximating the quantity $-rV(r)$ determined by Herman and Skillman.¹¹ The Herman-Skillman approximation starts with the Hartree-Fock-Slater treatment of atomic structure, but modifies it so that all the atomic orbitals are eigenfunctions of a common central potential. We approximate the quantity $-rV(r)$ by a series of straight lines; with this further approximation, the one-electron radial Schrödinger equation is exactly solvable in terms of Whittaker functions. Thus, we find orthonormal continuum orbitals as readily as discrete orbitals. The procedures used in determining the straight lines are given in Ref. 6. Comparison made in Ref. 6 with the calculations of Manson and Cooper¹² indicates that our straight-line approximation is accurate. However, for

elements heavier than Ar, both calculations indicate that for wavelengths near the optical threshold the calculated cross section is twice as large as experiment and it drops off faster with decreasing wavelength than experiment. This is due to the neglect, in a common central field approximation, of exchange and correlation effects.¹³ However, at larger energies (energies appropriate to the continuum orbital in these Auger transition calculations) the calculations and experiment agree to 20%, indicating that the one-electron orbitals are a good approximation.

Initially, each integral in the double integral of Eq. (1) was done by the trapezoidal rule with 100 steps. It was then found that 50-step integrals produced results agreeing with the initial results to better than one part in 100. The 50-step integrals were then used throughout. The grid was chosen such that at the outermost point in the $r_1(r_2)$ integration

$$\psi_{l_a}(\psi_{l_b})$$

was less than 10^{-4} of its maximum value.

Reference 11 provides central fields for neutral atoms only. To compute the central field for ions with inner-shell holes, we used the program given in Ref. 11. To check the sensitivity of the calculations to the precise form of the wave functions, we performed calculations using (1) neutral atom orbitals for both initial and final states, (2) orbitals for the atom with a 1s hole in both initial and final states, (3) orbitals for the atom with a 1s hole in the initial state, and 1s and continuum orbitals for the atom with two other holes as the final state. In procedure (3), we violate the unrelaxed core approximation used in deriving Eq. (1). We assume that the lack of orthogonality in the overlap integrals will add terms to Eq. (1). These we neglect. In addition, the expressions in Eq. (1) are modified by an overlap correction which is less than unity. Comparison of the three sets of orbitals were done for Mg and the experimental¹⁴ Auger continuum electron energies were used. We found that procedure (1) led to rates significantly smaller than (2) and (3); that (3) resulted in two electron matrix elements somewhat larger than (2), but when overlap corrections ($\sim 10\%$) were included (2) and (3) were substantially the same. Further, the continuum electron energy estimated from (2) (i. e. , $\epsilon_c = -\epsilon_{1s} + \epsilon_{n'l} + \epsilon_{n'l'}$) was close to the experimental value, and that the difference in the calculated matrix elements when using the

TABLE I. Herman-Skillman and model one-electron eigenvalues for the Mg and Ar ions (the neutral atom with a 1s hole). The Herman-Skillman eigenvalue is listed first.

Ion	$-\epsilon_{1s}$	$-\epsilon_{2s}$	$-\epsilon_{2p}$	$-\epsilon_{3s}$	$-\epsilon_{3p}$
Mg	103.8	8.90	6.67	1.29	
	102.9	9.00	6.63	1.29	
Ar	246.6	26.6	22.5	3.35	2.24
	245.5	27.4	22.7	3.45	2.24

estimated and experimental continuum electron energy was small. As a result, throughout these calculations we use orbitals appropriate to the atom with a 1s hole for both initial and final state.

In Table I, is listed the Herman-Skillman¹¹ and model eigenvalues for the Mg and Ar ions with a 1s hole. In Table II, we include the *KLL* Auger transition rates for Mg calculated with the experimental Auger continuum energies as well as model eigenvalues.

IV. CALCULATED VALUES

In Table II, the matrix elements and total Auger rate for *KLL* transitions are given; in Table III for *KLM*₁ transitions and in Table IV for *KLM*_{2,3}. In Table V, are listed the calculated oscillator

TABLE II. Matrix elements and total Auger rate for *KLL* transitions in Be–Ar. The units are inverse atomic time units (1 atu = 2.42×10^{-17} sec).

Element	$R_0(002s2s)$	$R_0(012s2p)$	$R_1(012p2s)$	$R_1(002p2p)$	$R_1(022p2p)$	A_{KLL}
Be	0.643×10^{-2}					
B	1.16	-0.849×10^{-2}	-1.23×10^{-2}			23.7×10^{-4}
C	0.860	-0.723	-1.16	-1.10×10^{-2}	2.68×10^{-2}	23.5
N	0.811	-0.679	-1.15	-1.05	2.69	34.4
O	0.815	-0.693	-1.14	-1.07	2.71	52.9
F1	0.809	-0.683	-1.12	-1.04	2.67	72.8
Ne	0.808	-0.675	-1.09	-1.01	2.60	94.8
Na	0.773	-0.687	-1.13	-1.02	2.64	97.1
Mg	0.899	-0.768	-1.20	-1.12	2.84	116
Al	0.878	-0.748	-1.18	-1.08	2.77	110
Si	0.646	-0.819	-1.32	-1.14	2.98	123
P	0.708	-0.844	-1.38	-1.27	3.27	143
S	0.692	-0.863	-1.36	-1.22	3.16	138
Cl	0.793	-0.907	-1.47	-1.37	3.49	164
Ar	1.03	-0.910	-1.45	-1.38	3.48	169
Mg(expt)	0.908	-0.779	-1.18	-1.15	2.91	
Ar (2→3)	3.87×10^{-4}	-1.23×10^{-4}	-6.06×10^{-4}	-8.77×10^{-4}	32.4×10^{-4}	0.95

TABLE III. Matrix elements and total Auger rate for KLM_1 transitions in Na–Ar. The units are inverse atomic time units ($1 \text{ atu} = 2.42 \times 10^{-17} \text{ sec}$).

Element	$R_0(0, 0, 2s3s)$	$R_0(003s2s)$	$R_0(013s, 2p)$	$R_1(012p3s)$	A_{KLM_1}
Na	$+0.464 \times 10^{-3}$	$+1.91 \times 10^{-3}$	-1.66×10^{-3}	-1.19×10^{-3}	1.11×10^{-4}
Mg	+0.190	+2.39	-1.99	-3.34	3.57
Al	+0.206	+2.58	-2.14	-3.63	4.14
Si	+1.03	+1.68	-2.14	1.47	4.96
P	+1.14	+2.16	-2.56	1.81	7.25
S	+1.34	+2.15	-2.68	1.92	7.90
Cl	+1.34	+2.39	-2.73	1.48	7.89
Ar	+1.40	+3.32	-2.86	2.15	10.2

TABLE IV. Matrix elements and total Auger rate for $KLM_{2,3}$ transitions in Al–Ar. The units are inverse atomic time units ($1 \text{ atu} = 2.42 \times 10^{-17} \text{ sec}$).

Element	$R_0(012s3p)$	$R_1(013p2s)$	$R_1(002p3p)$	$R_1(003p2p)$	$R_1(002p3p)$	$R_1(023p2p)$	$A_{KLM_{2,3}}$
Al	-1.65×10^{-3}	-3.15×10^{-3}	-4.65×10^{-3}	-2.87×10^{-3}	$+7.74 \times 10^{-3}$	$+7.04 \times 10^{-3}$	2.02×10^{-4}
Si	0.207	-3.66	+5.98	-3.05	+3.26	+7.86	4.82
P	0.226	-3.92	+1.14	-3.43	+8.11	+8.76	7.49
S	0.404	-4.10	-3.07	-3.51	+10.93	+8.91	13.2
Cl	0.370	-4.51	-3.17	-3.97	+11.82	+10.00	19.7
Ar	0.424	-4.38	-4.39	-3.99	+12.3	+9.90	25.0

TABLE V. Oscillator strength per electron for transition to a $1s$ hole, total radiative rate, total transition rate, and fluorescence yield for B–Ar. The units, except for the dimensionless fluorescence yield, are inverse atomic time units ($1 \text{ atu} = 2.42 \times 10^{-17} \text{ sec}$).

Element	f_{1s-2p}	f_{1s-2p}	$\sum A_R$	$\sum(A_R + A_A)$	ω_K
B	0.0377		0.0202×10^{-4}	23.7×10^{-4}	0.00085
C	0.0382		0.0824	23.6	0.0035
N	0.0373		0.225	34.6	0.0065
O	0.0377		0.520	53.4	0.0097
F	0.0368		1.04	73.8	0.0141
Ne	0.0360		1.79	96.6	0.0185
Na	0.0377		2.92	101.1	0.0289
Mg	0.0393		4.25	123.9	0.0343
Al	0.0382	0.00243	5.79	121.9	0.0473
Si	0.0420	0.00283	8.88	141.7	0.0627
P	0.0453	0.00322	13.0	170.8	0.0761
S	0.0435	0.00341	15.9	175.0	0.0909
Cl	0.0480	0.00388	24.0	215.6	0.111
Ar	0.0472	0.00370	29.8	234.0	0.127

strength per electron, the total radiative rate and the fluorescence yield. In addition, in Table II we list the matrix elements and total transition rate for KMM transitions in Ar. KMM transi-

tions contribute a negligible part of the total Auger rate and are neglected throughout.

In Fig. 1, the calculated fluorescence yields are shown along with the experimental results quoted

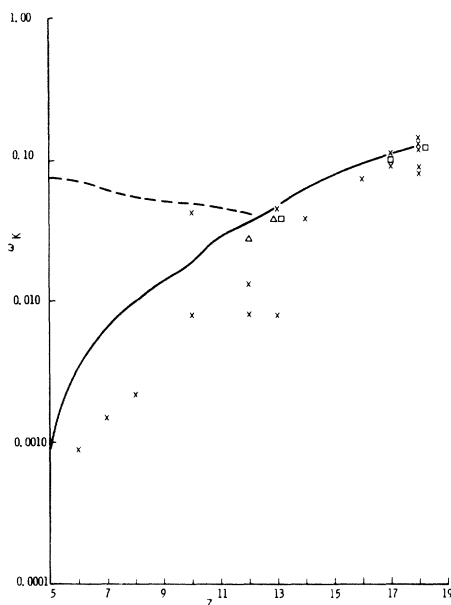


FIG. 1. K -shell fluorescence yield from B to Ar. The solid line connects the calculated yield for neutral atoms; the dotted curve connects the yield for AlII to AlIX. The \times 's are from Ref. 12, the Δ 's from Ref. 13, and the \square 's from Ref. 14.

in Fink *et al.*¹⁵ the recent results of Konstantinov *et al.*¹⁶ for Mg and Al, and Bailey and Swedlund¹⁷ on Al, Cl, and Ar. The calculated value is in good agreement with the measured value of Bailey and Swedlund for Ar and Cl, but about 25% too high for Al and Mg. For carbon, the calculated fluorescence yield is 0.0035. Khan, Potter, and Worley¹⁸ measure $\sigma_{1s}\omega_K$ for carbon as $2.24 \times 10^{-21} \text{ cm}^2$ at 1 MeV, where σ_{1s} is the ionization cross section. Using the calculated fluorescence yield, $\sigma_{1s} = 6.4 \times 10^{-19} \text{ cm}^2$. Born approximation calculations by the author¹⁹ indicate a cross section of $6.5 \times 10^{-19} \text{ cm}^2$. Watanabe²⁰ has fitted a one-electron model to the observed Ar K absorption near threshold. He determines a K -state width of 0.68 eV. Using $\tau = 1/\sum (A_R + A_A)$ and $\Delta E = \hbar/\tau$ we have $\Delta E(e - V) = 27.1/\tau(\text{atu})$. For Ar, our calculated value is $\Delta E = 0.634 \text{ eV}$, in reasonable agreement with Watanabe's values.

The discrepancy between the calculated and measured K -shell fluorescence yields for aluminum (25%) may be taken as an estimate of the accuracy of the calculation. To see the dependence of the fluorescence yield on the degree of initial ionization we have calculated ω_K for the ions AlII to AlIX. The calculated values are shown as the dotted curve in Fig. 1, where Z represents the number of electrons in the ground state of the ion before creation of the K hole. The calculation indicates that ω_K increases slowly with degree of

ionization, and that an extrapolation of the dotted curve to AlI would lead to a value of ω_K in excellent agreement with the measured value; thus, the estimate of accuracy.

V. COMPARISON WITH MEASURED AUGER INTENSITY RATIOS

KLL Auger transitions from filled shells lead to final-state ion configurations $(2s)^0(2p)^6$; $(2s)^1(2p)^5$; and $(2s)^2(2p)^4$. Asaad⁴ calls these configurations I, II, and III, respectively. Measurements and calculations of Auger intensities are often stated as ratios of the intensities of II and III relative to I. However, neglect of configuration interaction effects between I and III can lead to gross differences between measured and calculated ratios. This is largely due to changes in the intensity arising from configuration I. Asaad⁴ has recently discussed this situation, and corrected for configuration interaction. However, this correction does not significantly change the total intensity arising from configuration III. Thus, the ratio of total intensity arising from configuration III to that arising from configuration II is largely unaffected by configuration interaction.

In Fig. 2, we plot the ratio of calculated III to II values as a function of Z . Shown also are the ratios measured by Fahlman *et al.*¹⁴ for Na and Mg, Korber and Mehlhorn²¹ for Ne, and a mean

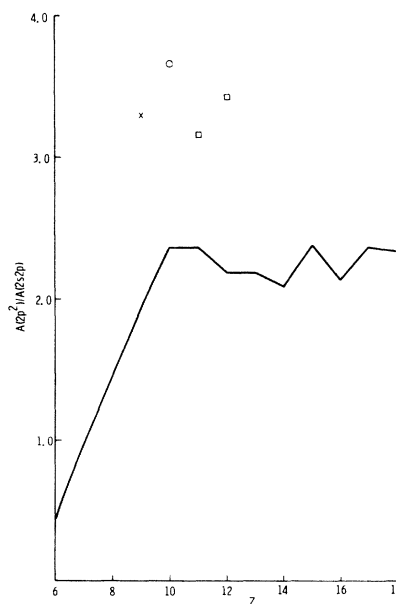


FIG. 2. Ratio of $(2p)^2$ Auger transition intensity to $(2p, 2s)$ intensity. The \times is from Ref. 19, the \circ from Ref. 18, and the \square 's from Ref. 8.

of measurements made by Albridge *et al.*²² on various fluorides. Not shown are the calculated values for AlII, AlIII, and AlIV with an initial 1s hole. They are 2.11, 2.21, and 2.24, respectively, while for AlI the ratio is 2.18. Thus while an extrapolation of the Al-ion-sequence fluorescence yield indicates an error of 25% in the AlI fluorescence yield, the ratios of intensity of configuration III to II remains approximately constant. Asaad,⁴ in correcting for configuration interaction between III and I in Ar, uses two different sets of computed matrix elements and finds the intensity ratio of configuration III to II to be 2.26 and 2.21. The experimental value is greater than 3.0. We find a ratio of 2.33 for Ar. But we also find the K-shell fluorescence yield for Ar to be in excellent agreement with experiment. Thus, the measurements of Auger intensity ratios are either in error, or there is a mechanism, besides configuration interaction, modifying the intensity of individual Auger transitions while keeping the total Auger rate constant. Considering the number of approximations in these calculations the latter possibility appears likely.

VI. CONCLUSIONS

Several approximations were made in these calculations. The use of time-dependent perturbation theory, the use of product-type wave functions and the unrelaxed core approximation to reduce the matrix element between initial and final states to tractable two-electron integrals and the approximation of the Herman-Skillman potential by one which leads to an exactly solvable

Schrödinger equation. The comparison of the calculated Al fluorescence yield with experiment and with the extrapolation of the Al-ion fluorescence yields led to an error estimate of 25%. It may be larger for elements lighter than Al and it is definitely smaller for heavier elements. This error appears to arise from the common central potential approximation since in stripping away outer electrons, as we did with the Al ions, we should be increasing the applicability of the common central-field approximation. With regard to the applicability of time-dependent perturbation theory, the calculated transition rates indicate that these transitions occur over periods more than 100 times than relevant characteristic atomic times. Thus, time-dependent perturbation theory appears to be a good approximation.

With regard to the second major approximation leading to two-electron integrals, the experimental evidence on individual Auger intensities seems to indicate a more sophisticated treatment is necessary. The total *KLL* Auger transition rate appears in good agreement with experiment (as indicated by the fluorescence yields) but the individual configuration intensities can differ from experiment by 50%. Asaad's⁴ correction for configuration interaction does not account for the discrepancy.

ACKNOWLEDGMENTS

The author wishes to thank Dr. J. M. Hoffman of this laboratory for suggesting this study, and Miss Ruth Lighthill, for providing the Herman-Skillman central fields.

*Work performed under the auspices of the U. S. Atomic Energy Commission.

¹P. Auger, *J. Phys. Radium* **6**, 205 (1925).

²E. H. S. Burhop, *The Auger Effect and Other Radiationless Transitions* (Cambridge University Press, Cambridge, England, 1952).

³E. J. Callen, *Phys. Rev.* **124**, 793 (1961).

⁴W. N. Asaad, *Nucl. Phys.* **66**, 494 (1965).

⁵R. A. Rubenstein, Ph.D. thesis, University of Illinois, 1955 (unpublished).

⁶E. J. McGuire, *Phys. Rev.* **175**, 20 (1968).

⁷N. F. Mott and H. S. W. Massey, *The Theory of Atomic Collisions* (Oxford University Press, London, England, 1949), 2nd ed.

⁸G. Racah, *Phys. Rev.* **63**, 367 (1943).

⁹E. J. McGuire, Sandia Research Report No. SC-RR-69-137 (unpublished).

¹⁰H. A. Bethe and E. E. Salpeter, *Quantum Mechanics of One- and Two-Electron Atoms* (Academic Press Inc., New York, 1957).

¹¹F. Herman and S. Skillman, *Atomic Structure Calculations* (Prentice-Hall, Inc., Englewood Cliffs, New

Jersey, 1963).

¹²S. T. Manson and J. W. Cooper, *Phys. Rev.* **165**, 126 (1968).

¹³J. W. Cooper, *Phys. Rev.* **128**, 681 (1962).

¹⁴A. Fahlman, R. Nordberg, C. Nordling, and K. Siegbahn, *Z. Physik* **192**, 476 (1966).

¹⁵R. W. Fink, R. C. Jopson, H. Mark, and C. D. Swift, *Rev. Mod. Phys.* **38**, 513 (1966).

¹⁶A. A. Konstantinov, V. V. Perepelkin, and T. E. Sazonova, *Izv. Akad. Nauk SSSR, Ser. Fiz.* **28**, 107 (1964) [English transl.: *Bull. Acad. Sci. USSR, Phys. Ser.* **28**, 103 (1964)].

¹⁷L. E. Bailey and S. B. Swedlund, *Phys. Rev.* **158**, 6 (1967).

¹⁸J. M. Khan, D. L. Potter, and B. D. Worley, *Phys. Rev.* **139**, A1735 (1965).

¹⁹E. J. McGuire (to be published).

²⁰T. Watanabe, *Phys. Rev.* **139**, A1747 (1965).

²¹H. Korber and W. Mehlhorn, *Z. Physik* **191**, 217 (1966).

²²R. G. Albridge, K. Hamrin, G. Johansson, and A. Fahlman, *Z. Physik* **209**, 419 (1968).